Experimental Investigation on Diethyl Carbonate Combustion

S.P. Cooper, C.M. Grégoire, Y.M. Almarzooq, E.L. Petersen, and O. Mathieu
J. Mike Walker '66 Department of Mechanical Engineering, Texas A&M University
College Station, Texas, USA

1 Introduction

Lithium-ion battery (LIB) fires are linked to the flammability of the electrolyte and pose not only a significant safety hazard due to the heat, but also the harmful chemicals that can be released during combustion [1]. Therefore, it is imperative to characterize the fundamental chemistry behind the electrolyte's flammability so strategies to prevent batteries from igniting can be designed. LIBs utilize an electrolyte mixture as a medium to exchange ions from one pole of the capacitor to another. This electrolyte medium consists of many different compounds, but are mainly comprised of carbonates both linear and cyclic [2]. One of these common solvents is diethyl carbonate (DEC), a symmetric ester of carbonic acid and ethanol taking the form shown in Fig. 1. Additionally, the chemical kinetics of DEC combustion is important from a transportation and propulsion perspective, as DEC is also an oxygenated additive candidate in diesel fuel [3].

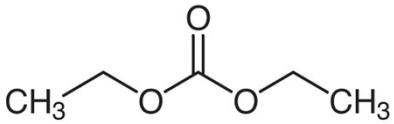

Figure 1: Molecular structure of diethyl carbonate (DEC).

Several recent studies have investigated the chemical kinetics of DEC combustion both experimentally and numerically, with ignition delay time (IDT) measurements from a rapid-compression machine [4] and a shock tube (ST) [4], laminar flame speed measurements (LFS) [5], speciation from jet-stirred reactors [4,5], flow reactor [6], shock tubes [7,8] and a micro flow reactor with a controlled temperature profile [9], as well as ab initio calculations for specific rate constants and reaction pathway identification [4,7]. However, a recent study on DEC pyrolysis from our group [8], where CO was followed using a laser absorption diagnostic, showed that the ethanol chemistry needed to be updated. Several modifications of the DEC mechanism (resulting in the TAMU model) allowed for significant improvements for the CO predictions. In the present study, the CO diagnostic is now applied to oxidative conditions, and the literature data are further complemented by IDT measurements in ST, and along with LFS data that were measured using spherically expanding flames in a constant-volume vessel at initial conditions of 403 K and 1 atm. These different experimental apparatuses are presented below before presenting the data and the comparisons with the TAMU mechanism as well as others from the literature.

Correspondence to: olivier.mathieu@tamu.edu

2 Experimental Methods

2.1. Shock Tubes

For the CO laser absorption experiments, the shock tube used has a driven inner diameter and length of 16.2 cm and 7.88 m, respectively. Five piezoelectric pressure transducers (PCB P113A22), over the last 2 m of the shock tube, were employed to detect shock passage and extrapolate the incident-shock velocity near the endwall. This velocity is then used to calculate the reflected-shock pressure and temperature to within an uncertainty of ±1% and ±0.8%, respectively. Pure helium was used as the driving gas. Two sapphire windows at the sidewall location, 1.6 cm upstream from the endwall, are mounted transversely to allow laser access. Further details on the AST have been provided previously [8].

The heated, high-pressure shock tube (HPST) facility at Texas A&M University was utilized to measure the ignition delay times for DEC. The HPST's driven section has an inner diameter of 15.24 cm and is 5.03 m in length. In contrast to the AST, the HPST uses four pressure transducers (PCB 113B22) over the last 1.44 m of the shock tube to collect three incident-shock-velocity measurements and extrapolate the shock velocity at the endwall location. Further details on the heating system and HPST can be found elsewhere [10]. Both shock tubes utilize 0.25-mm thick, polycarbonate diaphragms to initiate shock propagation. To facilitate ideal and repeatable diaphragm rupture, a cross-shaped cutting blade is used downstream of the diaphragm.

2.2. Optical Diagnostics

CO time histories were collected from mixtures diluted in 99.25% diluent (20% He, 79.25 % Ar) via transversely mounted window ports, 1.6 cm upstream from the endwall. A quantum cascade laser producing coherent light near 4.8 μm allowed access to the P(20) 1←0 transition band of CO at 2059.91 cm^{-1}. A separate cell containing a 10% CO, 90% Ar mixture was introduced into the beam's path to center the laser on this transition line prior to each experiment. Two detectors (InSb) fitted with bandpass filters for collection of incident and transmitted light intensities, respectively. Temperature predictions made by the TAMU model were used to account for temperature change during the experiment. Previous studies performed in similar conditions estimated the uncertainty in CO concentration to be within ±3.8%.

For the heated shock tube, IDT experiments with "fuel/air" mixtures were performed, and OH* chemiluminescence near 307 nm was observed at the sidewall and endwall locations of the shock tube using photomultiplier tubes (Hamamatsu 1P21) in custom housings equipped with UV filters (307 nm center, 10 nm FWHM). Ignition delay time is then defined by the difference between the time of shock reflection and the linear extrapolation to zero emission of the steepest increase of OH* emission at the endwall location. Significant pressure rise due to combustion was observed and can also be used to define ignition.

2.3. Flame Speed Vessel

A heated, stainless steel, constant-volume vessel was used to collect LFS data. The 25.8-L, cylindrical vessel has a 31.8-cm internal diameter and is 28-cm in length. Optical access in this vessel is available through two opposing, 12.7-cm diameter, glass windows which allow for measurement of the LFS under near-constant-pressure conditions. A more detailed description of the vessel can be found in Krejci et al. [11]. A custom-fit heating jacket, which can produce a uniform temperature of up to 600 K, was used to heat the vessel to avoid fuel condensation. For the present study, the initial temperature and pressure were 403 K and 1 atm, respectively. A Photron Fastcam SA1.1 camera, with a rate of 10,000 fps, was used in a Z-type schlieren imaging setup to capture the spherically-propagating flame. The collected images were then analyzed using an in-house Python code for edge detection and the LFS was then calculated using the non-linear equation developed by Chen [12]. A known mass of fuel was introduced

to the vessel by injection using a syringe, and the resulting partial pressure of fuel was then recorded using a 0-100 Torr pressure gauge. After complete evaporation of the fuel, the vessel is filled with synthetic air to 1 atm. The resulting uncertainty in LFS using this experimental setup has been shown previously to be within ±1%; however, for the current study, a conservative ±5% is adopted. Gases used for both shock-tube and LFS experiments were obtained from Praxair with 99.999% purity and the fuel, obtained from Sigma-Aldrich, had an anhydrous purity of ≥ 99%.

3 Results

DEC ignition delay times collected near atmospheric pressure over a range of temperatures between 1182 and 1406 K behind reflected shock waves are shown in Fig. 2 for (a) $\phi = 0.5$, (b) $\phi = 1.0$, and (c) $\phi = 2.0$. As can be seen, the evolution of the ignition delay time with the temperature follows the classical evolution observed for hydrocarbons at high temperature. Models offer similar predictions (within a factor of 2 typically) and are predicting the experimental results with good accuracy overall, within the experimental uncertainty for the most part. The global activation energy (corresponding to the slope of the model) tends to be slightly higher for the model than what is observed experimentally. This higher activation energy leads to divergences between the models and the data below 1250 K for the (b) stoichiometric and (c) fuel-rich cases. Note that the difference between the data and model on the low-temperature side is not due to inhomogeneous ignition in the shock tube, but to the model's predictions.

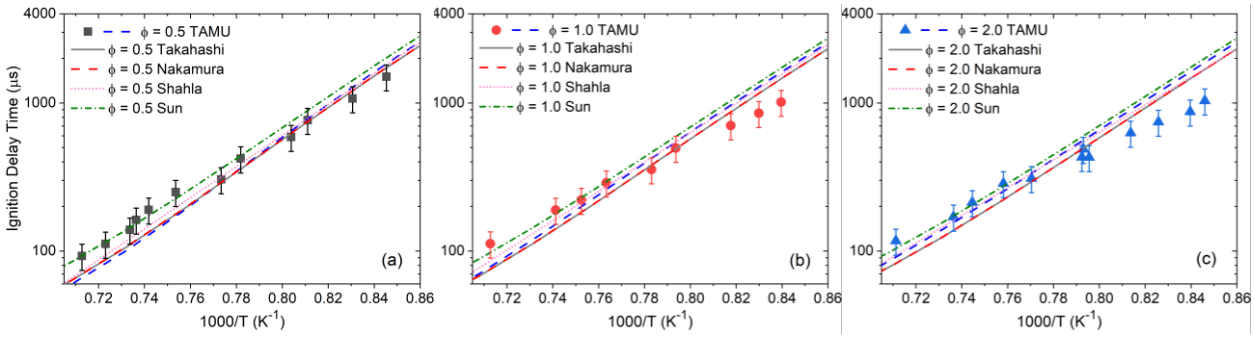

Figure 2: IDT for DEC/air mixtures at (a) $\phi = 0.5$, (b) $\phi = 1.0$, (c) $\phi = 2.0$, and comparison with model predictions.

The laminar flame speed results obtained during this study are visible in Fig. 3, where the classical curve peaking at around $\phi = 1.1$ is obtained. The maximum laminar flame speed obtained experimentally is 55.6 cm/s, at 403 K and 1 atm for the initial conditions. As one can see in Fig. 3, the models considered herein are all within the experimental uncertainty (which appears large only because the y axis of the graph ranges between 40 and 60 cm/s), but they all fall under the experimental measurements. Among these models, the TAMU, Shahla, and Nakamura models are the closest to the data. They also present nearly identical predictions for stoichiometric and fuel-rich mixtures. At fuel-lean conditions, the Shahla model offers marginally better predictions.

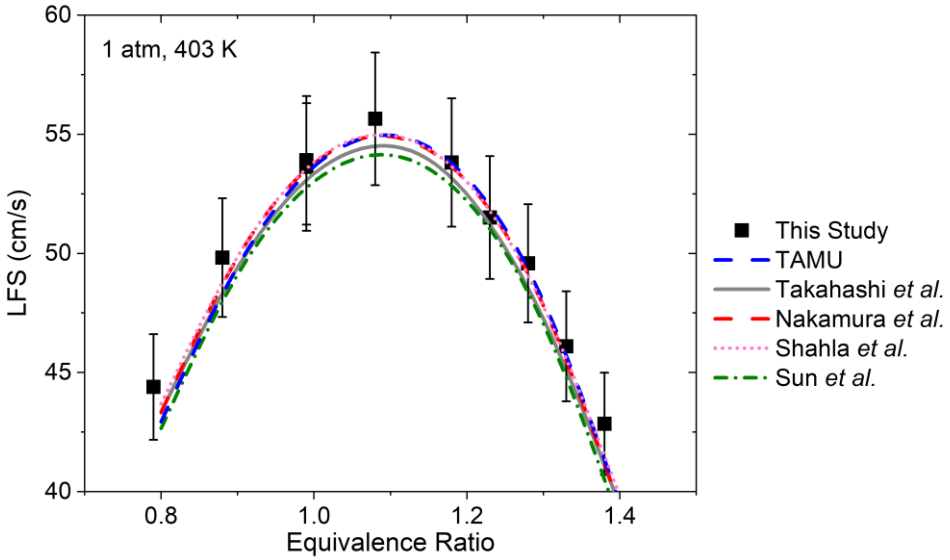

Figure 3: Laminar flame speed results from this study at initial conditions of 1 atm and 403 K compared to model predictions from the present study and those from the literature.

Experiments conducted under high dilution (79.25% Ar and 20% He) at fuel lean (a-c), stoichiometric (d-f) and fuel-rich (g-i) cases are shown in Fig. 4 for high-, mid-, and low-temperature conditions. As one can see, for the high- and medium-temperature cases for the fuel-lean and stoichiometric mixtures, a peak in the CO concentration is reached after a delay that increases when the temperature decreases. After this initial rapid formation of CO, the carbon monoxide concentration decreases with time due to the oxidation of CO into CO_2. On the other hand, for the fuel-rich case, the peak is not as well defined, and the CO reaches a plateau level. This plateau is to be expected and is typically observed for mixtures when the oxygen concentration is insufficient to fully oxidize the fuel.

Concerning the models, the shape of the profiles and experimental trends are well captured by all models for the fuel-lean and stoichiometric cases. Little difference is seen between the models by Nakamura, Sun, and Takahashi, each basically builds on the earlier, but little change is observed for the CO concentration measurements. The CO concentration at the peak tends to be over-estimated by 10-15% by these models, and they also tend to be slightly over-reactive for the fuel-lean condition. At fuel-lean conditions, the Shahla model presents very similar predictions to those models but is however in better agreement with the time-to-peak timing observed for the experiments at $\phi = 0.5$ (Fig. 4b). Lastly for the fuel-lean and stoichiometric mixtures, the TAMU model predicts lower levels of CO at the peak, in better agreement with the experimental data, but this model is also more reactive, which induces a peak CO found earlier than the experimental one, notably at intermediate temperatures. For the fuel-rich case, the experimental profile at high temperature (Fig. 4g) is not captured by the models, and the CO level at the plateau is significantly over-predicted by nearly 50%. At intermediate temperatures (Fig. 4h), the shape is better predicted (at least during the timeframe of the experiment) and the TAMU model is still over-reactive (all the other models being extremely close in terms of predictions). However, at this condition, the difference between the models and the experimental profile is only 20-25% for the CO concentration. This result is rather surprising for the TAMU model, as it predicts much smaller concentration of CO compared to the other models in pyrolysis condition. Thus, the results of the present study seem to indicate the presence and preference of an alternative route for CO formation that uses the O_2 present in the mixture.

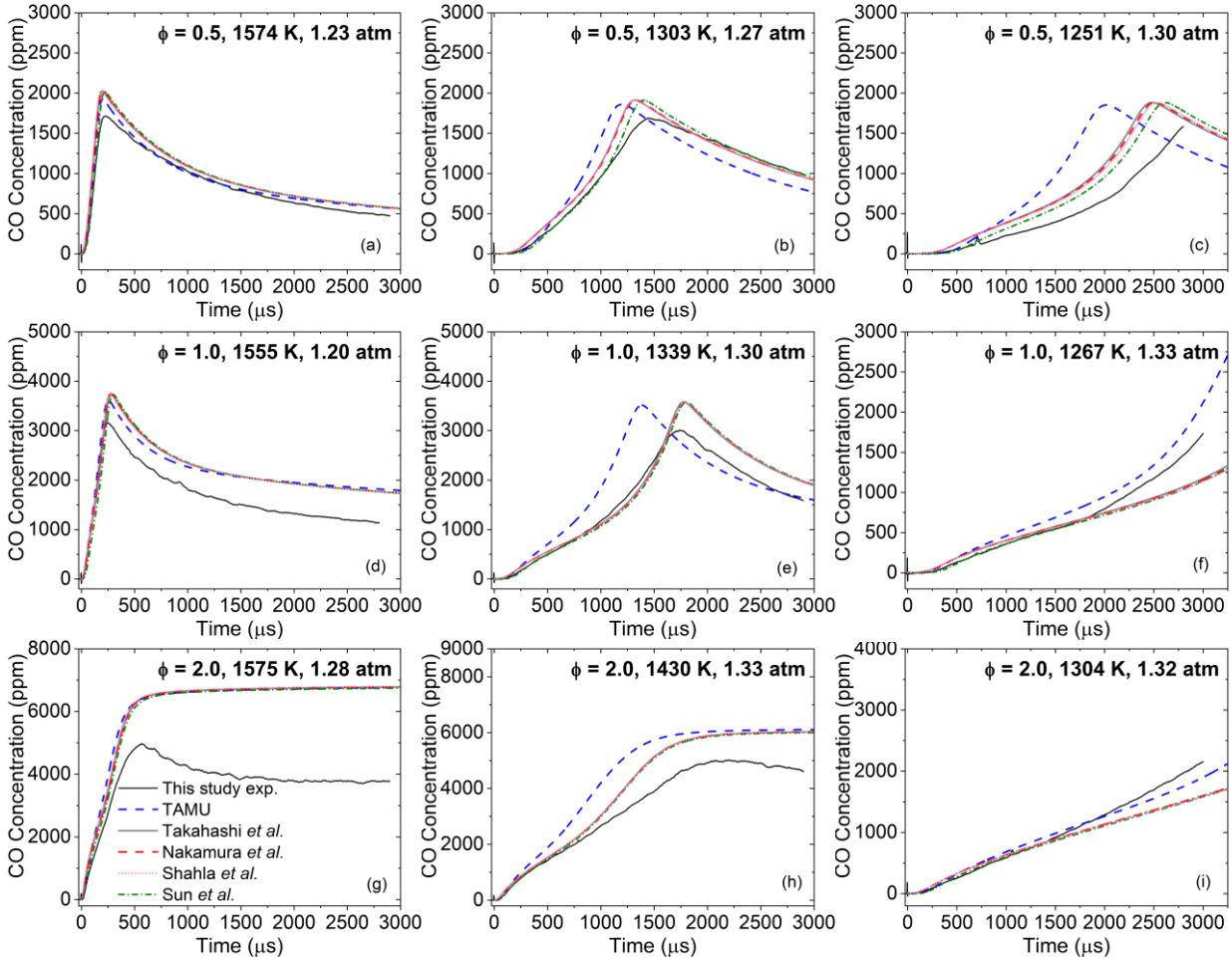

Figure 4: High-, mid-, and low-temperature traces (left to right) for ϕ = 0.5 (a-c), 1.0 (d-f) and 2.0 cases (g-I, top to bottom). Modeling results are also shown for the mechanism from the present study (bold blue dashes), as well as those from Nakamura et al. (red dashes), Sun et al. (green dash-dots), Shahla et al. (pink dots), and Takahashi et al. (grey line).

4 Conclusions

The combustion chemistry of DEC was investigated experimentally by measuring a large variety of combustion parameters such as ignition delay time, laminar flame speed, and CO time histories over a wide range of conditions and near-atmospheric pressure. These results were compared with detailed kinetics models from the literature, and the comparison shows that the global kinetics data (ignition delay time and laminar flame speed) are accurately predicted by all models considered. On the other hand, the kinetics measurement of CO showed room for improvement for the models. A numerical analysis was conducted, and this analysis exhibited a complex chemistry, with several pathways involved at different times. It is likely that the CO formation from C2 species, notably C_2H_4, as described in the models is the reason behind the inaccurate predictions during DEC combustion. The authors believe that a complementary shock tube, laser-absorption based study of the CO formation during C_2H_4 oxidation would be necessary to clarify and possibly solve this issue.

5 Acknowledgments

The authors would like to thank the National Science Foundation for the financial support of this study (award # 2037795). Additional support came from the TEES Turbomachinery Laboratory through a Ralph-James Fellowship for C.M.G. and from King Saud University (KSU) through Saudi Arabian Cultural Mission (SACM) fellowship# 4/52/60746 for Y.M.A.

References

[1] Larsson F, Andersson P, Blomqvist P, Mellander BE. (2017). Toxic fluoride gas emissions from lithium-ion battery fires. Scientific reports 7: 1.

[2] Li Q, Chen J, Fan L, Kong X, Lu Y. (2016). Progress in electrolytes for rechargeable Li-based batteries and beyond. Green Energy & Environment 1: 18.

[3] Aguado-Deblas L, Hidalgo-Carrillo J, Bautista FM, Luna C, Calero J, Posadillo A, Romero AA, Luna D, Estévez R. (2020). Biofuels from diethyl carbonate and vegetable oils for use in triple blends with diesel fuel: Effect on performance and smoke emissions of a Diesel engine. Energies 13: 6584.

[4] Nakamura H, Curran HJ, Córdoba AP, Pitz WJ, Dagaut P, Togbé C, Sarathy SM, Mehl M, Agudelo JR, Bustamante F. (2015). An experimental and modeling study of diethyl carbonate oxidation. Comb. Flame 162: 1395.

[5] Shahla R, Togbé C, Thion S, Timothée R, Lailliau M, Halter F, Chauveau C, Dayma G, Dagaut P. (2017). Burning velocities and jet-stirred reactor oxidation of diethyl carbonate. Proc. Comb. Inst. 36: 553.

[6] Sun W, Huang C, Tao T, Zhang F, Li W, Hansen N, Yang B. (2017). Exploring the high-temperature kinetics of diethyl carbonate (DEC) under pyrolysis and flame conditions. Comb. Flame 181: 71.

[7] Sela P, Zhang Y, Herzler J, Fikri M, Schulz C, Peukert S. (2021). Pyrolysis of diethyl carbonate: Shock-tube and flow-reactor measurements and modeling. Proc. Comb. Inst. 38: 987.

[8] Grégoire CM, Cooper SP, Khan-Ghauri M, Alturaifi SA, Petersen EL, Mathieu O. (2023). Pyrolysis Study of Dimethyl Carbonate, Diethyl Carbonate, and Ethyl Methyl Carbonate using Shock-Tube Spectroscopic CO Measurements and Chemical Kinetics Investigation, Comb. flame 249: 112594.

[9] Kanayama K, Takahashi S, Morikura S, Nakamura H, Tezuka T, Maruta K. (2022). Study on oxidation and pyrolysis of carbonate esters using a micro flow reactor with a controlled temperature profile. Part I: Reactivities of dimethyl carbonate, ethyl methyl carbonate and diethyl carbonate. Comb. Flame 237: 111810.

[10] Cooper SP, Mathieu O, Schoegl I, Petersen EL. (2020). High-pressure ignition delay time measurements of a four-component gasoline surrogate and its high-level blends with ethanol and methyl acetate, Fuel 275 118016.

[11] Krejci MC, Mathieu O, Vissotski AJ, Ravi S, Sikes TG, Petersen EL, Kérmonès A, Metcalfe W, Curran HJ. (2013). Laminar Flame Speed and Ignition Delay Time Data for the Kinetic Modeling of Hydrogen and Syngas Fuel Blends. J. Engineer. Gas Turbines Power 135: 021503.

[12] Chen, Z. (2011). On the extraction of laminar flame speed and Markstein length from outwardly propagating spherical flames. Comb. Flame 158: 291.